ARTICLE

C$_2$H$_2$ Overtones Near 12300 cm^{-1} Revisited with a Very Sensitive Cavity Ring-down Spectrometer†

Bo Gao, An-wen Liu, Rui-xue Wu, Wei Ning, Shui-ming Hu*

Hefei National Laboratory for Physical Sciences at the Microscale, University of Science and Technology of China, Hefei 230026, China

A cavity ring-down spectrometer (CRDS) is constructed with a single-mode continuous-wave Ti:Sapphire laser. It allows attaining a minimum detectable absorption of 1.8×10^{-10} cm^{-1}. The spectrometer is applied to record the overtone spectrum of ^{12}C$_2$H$_2$ in the 12240−12350 cm^{-1}. Compared with the previous CRDS and intra-cavity laser absorption spectroscopy studies in the same region, the present measurement achieved better sensitivity and better precision as well. As a result, the ro-vibrational parameters of the high overtone bands of acetylene at 12290.12, 12311.82, and 12350.61 cm^{-1} have been refined. The advantages of the present CRD spectrometer is also demonstrated by the newly observed and well characterized perturbation on the f component of the very weak band near 12289 cm^{-1}. The quantitative measurement capability of the spectrometer is verified with the measurement of the water lines and employed to give the absolute band intensities of those three acetylene bands.

Key words: Near-IR, Cavity ring-down, C$_2$H$_2$, Overtone spectrum

I. INTRODUCTION

Direct absorption method is often preferable to measure the molecular spectra since one can straightforwardly retrieve absolute line intensities (or sample densities) from the spectra. However, the sensitivity is limited by the effective absorption length which rarely excesses several hundred meters with traditional multipass configuration. Cavity ring-down spectroscopy (CRDS) has been introduced as a very sensitive direct absorption based spectroscopy method [1]. The fundamentals of the technique and its different experimental implementations have been reviewed in many publications [2−7]. The main idea of this method is to measure the decay rate of the light (often laser) inside a resonant cavity composed of two high-reflectivity mirrors. The decay rate $1/\tau$, where τ is the "ring-down time", is proportional to the total optical losses inside the cavity. The sample absorption coefficient, α, can be derived from

$$\alpha = \frac{1}{c}\left(\frac{1}{\tau} - \frac{1}{\tau_0}\right) \tag{1}$$

where c is the speed of light, τ and τ_0 are the decay time of the cavity with and without sample, respec-

tively. In this case, the minimum detectable absorption loss (MDAL) can be derived from the minimum detectable change in the decay time, $\delta\tau_0$:

$$\alpha_{\min} = \frac{1}{c\tau_0{}^2}\delta\tau_0 \tag{2}$$

The pioneer CRDS implementations used pulsed lasers to inject light into the cavity. Beside the limited spectral resolution because of the pulsed-laser, the sensitivity of pulsed-CRDS is limited by multiple longitudinal modes excitation in the cavity. The first demonstration of continuous wave (cw)-CRDS is performed by Romanini *et al.* [8−10]. The narrow line width (several MHz or less) of the cw-laser allows to couple the laser mode to a single longitudinal mode of the ring-down cavity, thereby reducing the variations among different ring-down events. A noise equivalent MDAL of 2×10^{-10}/cm, which is the best CRDS sensitivity reported to date, has been obtained by using a diode laser operating at 1.5 µm wavelength and a couple of mirrors with reflectivity $R\approx99.999\%$ [9].

In this work, we report our recent built CRD spectrometer employing a widely tunable (0.7−1.0 µm) cw Ti:Sapphire laser in the near-IR region. As a demonstration, we recorded the spectroscopy of the overtone spectrum of ^{12}C$_2$H$_2$ in the region of 12240−12350 cm^{-1}. This region has been studied by CRDS [11] and intra-cavity laser absorption spectroscopy (ICLAS) [12] before and the result will be compared with previous CRDS and ICLAS studies in terms of sensitivity and spectral precision.
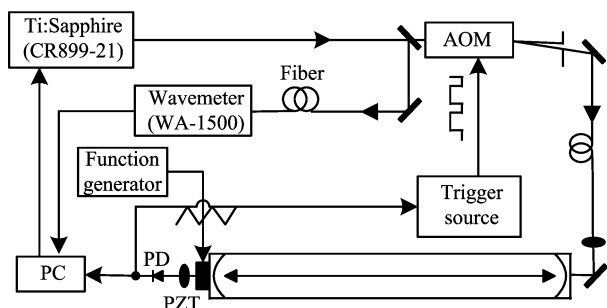
FIG. 1 Schematic diagram of the experimental setup. The abbreviations are as: acousto-optical modulator (AOM), personal computer (PC), photo detector (PD), piezo transformer (PZT).

II. EXPERIMENTS

The experimental setup is presented in Fig.1. The near-IR laser beam from a cw tunable Ti:Sapphire laser (Coherent 899-21) pumped with a 532 nm solid state laser (Coherent Verdi-18) first goes through an acoustic-optical modulator (AOM, ISOMET 1205C) then is coupled into a single-mode fiber. Using a set of lenses, the TEM00 mode of the laser beam is sent to a ring-down cavity. The cavity is 1.25 m long ended with a pair of high reflectivity (HR) mirrors. The two HR mirrors, curvature radius of 100 cm, were bought from Los Gatos Inc. and the stated reflectivity is 99.995%. One HR mirrors is mounted on a piezoelectric actuator (PI Inc.). The piezoelectric actuator is driven with a triangle wave from a function generator.

The Ti:Sapphire laser is running in a step-scan mode controlled by a personal computer (PC). On each step, without any change of the laser wavelength in a period of about 0.5 s, the cavity length is modulated with a 300 Hz triangle wave. Once the cavity longitude mode gets resonant with the laser frequency, in other word, a ring-down event occurs, the photo-current signal from the photodiode detector (PD) will increase dramatically and trigger a rectangular pulse driving the acousto-optical modulator (AOM) to chop the input laser radiation. The photo-current signal then decays exponentially and it will be recorded by a fast digitizer (ADLINK PCI-9820) installed in a personal computer. The digitizer is working at a sampling rate of 1 MS/s (Mega-samples per second) with 14-bit resolution. The total digitizer acquisition time is more than 7 times of the typical ring-down lifetime, as long as the signal amplitude exceeds the noise level.

Methods of the analysis of single exponential curves have been extensively reviewed by Istratov and Vyvenko [13]. The nonlinear Levenberg-Marquadt (LM) method offers the best performance in terms of accuracy and precision, but the fitting procedure is rather slow. Halmer *et al.* introduced a fast approach (the corrected successive integration (CSI)) in 2004, which was

based on the method of successive integration and corrected the systematic error of trapezoidal integration [14]. Mazurenka *et al.* introduced another approach which is based on fast fourier transform (FFT) analysis [15]. The two methods show comparable performance to the nonlinear LM method, but much faster since they are non-iterative methods. Here we adopted the CSI method because it is straightforward and easy for programming. The repetition rate of the ring-down events is typically 500 Hz. At one laser wavelength, about 100 ring-down events will be accumulated and the decay time values retrieved from fitting each of the decay curve will be averaged to reduce the noise level.

A λ-meter (Burleigh WA-1500) is used to measure the wavelength of the laser with an accuracy of ± 0.002 cm^{-1}. A Fabry-Perot Etalon is also used to monitor the laser frequency. The absolute calibration of the spectrum is carried out with the water lines given in HITRAN database [16].

III. OVERTONE SPECTROSCOPY OF $^{12}C_2H_2$

The acetylene sample was bought from the Nanking Special Gas Co. with a stated purity of 99.6%. The sample was further purified with the froze-pump-thaw method before use. The sample gas pressure is measured by a capacitance gauge of 0.5% full-scale accuracy. 9.28 kPa sample was filled in the cell. All spectra were recorded at room temperature (297$\pm$1 K).

In the studied spectral region, 12240−12350 cm^{-1}, three Π_u-Σ_g^+ transitions could be detected. Two stronger bands at 12311 and 12349 cm^{-1} had been reported by Halonen's group using a CRD spectrometer [11] and we have presented the additional weaker one at 12289 cm^{-1} using ICLAS [12]. The vibrational upper states of these three bands are univocally assigned to the {$N_s=v_1+v_2+v_3=4$, $N_r=5v_1+3v_2+5v_3+v_4+v_5=19$, $k=l_4+l_5=1$, u} polyad in a very good agreement with the predictions from the polyad model [17]. As illustrated in the spectrum shown in Fig.2 and Fig.3, the typical noise level is 1.8×10^{-10}/cm, which gives a sensitivity over 10 times better than previous CRDS measurement in the same region. A comparison with the ICLAS result [12] is also given in Fig.3. It is obvious that the present CRD spectrum is superior in terms of sensitivity (with lower noise level) and precision (with more symmetric line profile and narrower line width). For illustration, a simulation of the water lines in this region is also presented in Fig.2 using the data from HITRAN [16]. The Q-branch of the 12290 cm^{-1} band can be readily assigned. Note that there are quite a few strong water lines in this region. In the CRDS measurement, the water vapor presents as minor contamination in the sample and can be well reduced, however in the ICLAS measurement, since the laser cavity is unavoidably exposed in the air, the air broadened strong water lines often prevent the observation of the spectrum
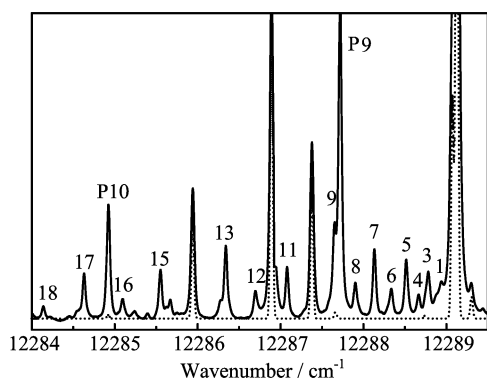
FIG. 2 The Q-branch of the Π_u-Σ_g^+ bands centered near 12289 cm^{-1}. The dotted line is simulated water spectrum with the data from the HITRAN database [16]. The lines marked by P9, P10 correspond to the the lines of the band near 12311 cm^{-1}.
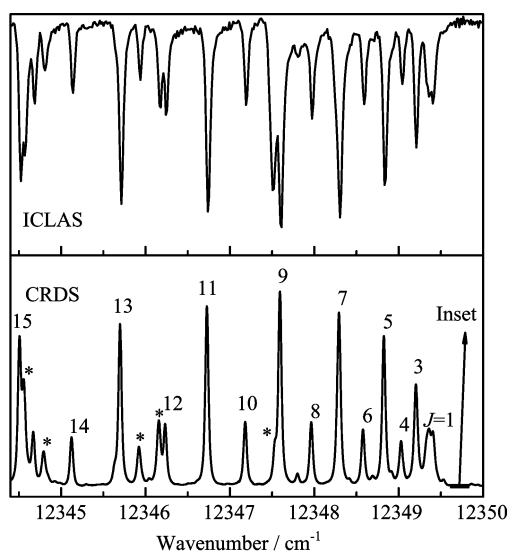

FIG. 3 Comparison of the ICLAS spectrum (upper) and present CRDS spectrum (lower) of the Q-branch of $^{12}C_2H_2$ band near 12349 cm^{-1}. The inset shows the CRDS spectrum noise level of 1.8×10^{-10}/cm. The peaks marked by stars are water vapor lines which have been given in the HITRAN database [16].

nearby. This is also an advantage of CRDS over ICLAS which will particularly affect the following analysis of this weak band.

The rotational assignments were carried out using the ground state combination differences (GSCD) method. The line positions were then fitted on the basis of the standard formula of the energy levels:

$$T_v = G_v(v_1, v_2, v_3, v_4^{l_4}, v_5^{l_5}) + F_v(J) \qquad (3)$$

$$F_v(J) = B_v[J(J+1) - k^2] - D_v[J(J+1) - k^2]^2 \quad (4)$$

where G_v and F_v are the vibrational and rotational contributions, respectively, and $k=l_4+l_5$ is the quantum number associated to the total vibrational angular mo-
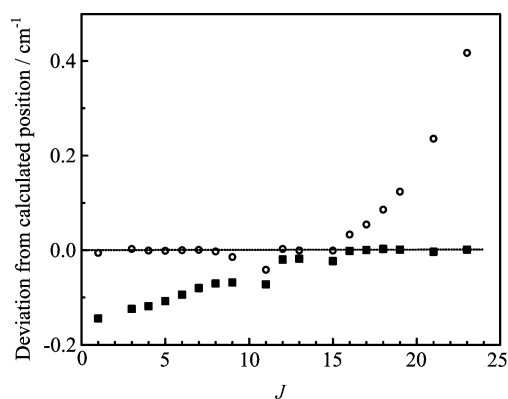

FIG. 4 Difference between the observed and calculated line positions of the f component of the Π_u state of $^{12}C_2H_2$ centered at 12288.963 cm^{-1}. with the values calculated using the spectroscopic parameters of Table I. versus the J rotational quantum number. Energy levels crossing observed around J=15 is due to perturbation from a dark state. Two fitting results are presented: (i) the open circles correspond to fitting of J<15 lines, leading to the parameters values listed in Table I, (ii) the full squares correspond to fitting of J>15 lines.

mentum. In the fitting procedure, the rotational constants of the ground state, B'' and D'', were constrained to their literature values [18] and the quantities ν_0, ΔB, and ΔD were fitted. The $\Pi(e)$ and $\Pi(f)$ components were fitted separately, leading to effective values of the spectroscopic parameters. The retrieved spectroscopic parameters are listed in Table I. Owing to the good signal-noise-ratio and the spectral precision, we can observe perturbation for the rotational levels of the f component of the Π_u vibrational state at 12288.963 cm^{-1}. The onset of the perturbation is at the level J'=16. No perturbation is found to the e component of the same vibrational state. So it is properly due to coriolis-type interaction from an unidentified dark state. The spectroscopic parameters for this band, listed in Table I, were derived with lines of $J'\leq15$. As illustrated by the deviations from the calculated line positions presented in Fig.4, a different set of ro-vibrational constants can be obtained by a fit including only higher J' lines (J'>15). It leads to a difference of 0.141 cm^{-1} between the two effective values of the vibrational term. As a comparison, due to lower sensitivity and accuracy, the previous CRDS measurement [11] has not observed this band, the ICLAS measurement [12] has not discriminate the perturbation reported here. For comparison, the previous CRDS and ICLAS results are also given in Table I, one can find that the present results show better precision and give more lines with higher J values.

To demonstrate the quantitative measurement capability of the present CRD spectrometer, the line intensities of the lines obtained in the measurement have also been retrieved from the spectra. The line strength of several well-isolated water lines were retrieved from the

TABLE I Rovibrational parameters (in cm^{-1}) of the Π_u-Σ_g^+ bands of $^{12}C_2H_2$ near 12300 cm^{-1}.

Band	v_0	G_v[b]	B_v	$D_v \times 10^6$	J_{MAX} (P/Q/R)	n/N[c]	rms[d]
(00000)Σ_g^{+}[a]		0.0	1.176646	1.62710			
Π_u(e)	12288.96260 (45)	12290.11819 (45)	1.15559 (16)	−5.678 (87)	14/ /11	16/20	0.77
Π_u(f)	12288.9633 (17)	12290.1249 (17)	1.161589 (41)	−1.89 (17)	/23/	9/19	2.1
Π_u(f) [12]	12288.9766 (36)	12290.1343 (36)	1.1581911 (47)	−7.60 (27)	13/17/11	18/25	3.6
Π_u(e)	12310.67081 (82)	12311.82265 (82)	1.151842 (23)		21/ /19	25/35	2.6
Π_u(e) [12]	12310.6705 (12)	12311.8223 (12)	1.151816 (17)	0.028 (43)	21/ /15	30/35	3.6
Π_u(e) [11]		12311.8152 (17)	1.151899(32)	0.37 (12)		/26	3.6
Π_u(f)	12310.66628 (41)	12311.82264 (41)	1.1563630 (23)	1.275 (19)	/35/	20/27	1.1
Π_u(f) [12]	12310.6667 (12)	12311.8231 (12)	1.156359 (12)	1.277 (22)	/27/	21/25	3.1
Π_u(f) [11]		12311.8228 (15)	1.156326 (19)	1.246 (43)		/26	3.5
Π_u(f)	12349.45130 (57)	12350.60739 (57)	1.1560910 (35)	1.6797 (38)	/31/	23/27	1.2
Π_u(f) [12]	12349.4493 (22)	12350.6054 (22)	1.1561222 (76)	1.727 (11)	/27/	21/24	2.2
Π_u(f) [11]		12350.6023 (17)	1.156085 (27)	1.616 (74)		/19	3.8

[a] Ground state constants from Kabbadj *et al.* [18].
[b] Band center defined as: $\nu_0 = G_{v'} - G_{v''} + B''l''^2 - B'l'^2$.
[c] n: number of transitions included in fitting; N: number of assigned rotational transitions.
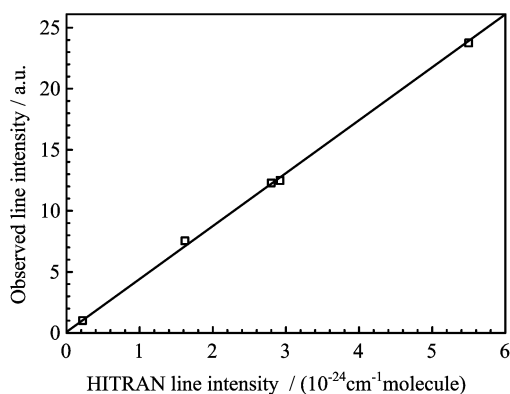[d] Root mean square deviation in 10^{-3} cm^{-1}.

FIG. 5 Water line intensities obtained from present CRDS measurement and those given in HITRAN database [16].

spectrum using a least-square fitting procedure where the line profile parameters (here Doppler-induced Gaussian width only) were fixed at calculated values. To test the consistency, the intensity values of these water lines are compared with that from the HITRAN database [16]. Since here water vapor was presented in our sample cell as contamination, we can not experimentally determine the pressure of the water vapor, so we just show the observed relative line intensities in Fig.5. It shows good linearity over a large range with water line intensity varying from 0.2×10^{-24} cm^{-1}molecule^{-1}) to 5.5×10^{-24} cm^{-1}molecule^{-1}). The linear fitting shown on the figure presents an accuracy of the relative intensity values as better than 5%.

Using the same line strength retrieval procedure, we obtained the line strength values (in 101 kPa^{-1}cm^{-2} at 296 K) of unblended lines in each of the three bands ob-served in this work. According to the following equation [19],

$$S_J = A\frac{\tilde{\nu}C}{QT}g'' \exp\left(-\frac{hcE''}{k_BT}\right) \cdot$$
$$\left[1 - \exp\left(-\frac{hc\tilde{\nu}}{k_BT}\right)\right]|R_J|^2 \qquad (5)$$

the modulus square of the transition dipole moment $|R_J|^2$ of each line can be determined. In Eq.(5), A is a constant equal to 308.52 MPa^{-1}cm^{-1}D^{-2}, $\tilde{\nu}$ is the wavenumber of the line, T is the sample temperature in Kelvin, E'' and g'' are the energy and degeneracy (including the statistical weight) of the lower level involved in the transition, $C=977.828 \times 10^{-3}$ is the isotopic abundance of $^{12}C_2H_2$ which is proposed by HITRAN [16], and Q is the total internal partition sum, which can be obtained from Ref.[20]. The constants h, c, and k_B are the Planck constant, the speed of light, and the Boltzman constant, respectively. The vibrational transition moment $R_{v'v}$ can be obtained through $|R_J|^2 = |R_{v'v}|^2 L_J$, if we neglect the vibration-rotation interactions. L_J is the Hönl–London factor. For the Π_u-Σ_g^+ transitions discussed here, $L_J = (J-1)/2$, $(2J+1)/2$, and $(J+2)/2$ for P, Q, and R branch, respectively [21]. In this case, the vibrational transition moment $|R_{v'v}|^2$ values (in Dedye^2) can be determined as $2.40(57) \times 10^{-11}$, $1.95(72) \times 10^{-10}$, and $1.26(33) \times 10^{-10}$ for the bands at 12289, 12311, and 12349 cm^{-1}, respectively. Note for the weakest band at 12289 cm^{-1}, the vibrational transition moment had not been given in previous ICLAS measurement due to lower sensitivity and overlapping with air-broadened water lines.

IV. CONCLUSION

A continuous-wave CRD spectrometer is built using a wide tunable Ti:Saphire laser. It is utilized to detect the acetylene overtone bands near 12300 cm^{-1}. Compared with the previous CRD and ICLAS measurements in the same region, the present result shows better sensitivity and accuracy, which leads to a refined ro-vibrational parameters of three ^{12}C$_2$H$_2$ bands in this region.

V. ACKNOWLEDGMENTS

[1] A. O'Keefe and D. A. G. Deacon, Rev. Sci. Instrum. **59**, 2544 (1988).

[2] S. M. Ball and R. L. Jones, Chem. Rev. **103**, 5239 (2003).

[3] G. Berden, R. Peeters, and G. Meijer, Int. Rev. Phys. Chem. **172**, 565 (2000).

[4] S. S. Brown, Chem. Rev. **103**, 5219 (2003).

[5] J. J. Scherer, J. B. Paul, A. O'Keefe, and R. J. Saykally, Chem. Rev. **97**, 25 (1997).

[6] M. Mazurenka, A. J. Orr-Ewing, R. Peverallb, and G. A. D. Ritchieb, Annu. Rep. Prog. Chem. C **101**, 100 (2005).

[7] B. A. Paldus and A. A. Kachanov, Can. J. Phys. **83**, 975 (2005).

[8] D. Romanini, A. Kachanov, N. Sadeghi, and F. Stoeckel, Chem. Phys. Lett. **264**, 316 (1997).

[9] D. Romanini, A. Kachanov, and F. Stoeckel, Chem. Phys. Lett. **270**, 538 (1997).

[10] D. Romanini, A. Kachanov, and F. Stoeckel, Chem. Phys. Lett. **270**, 546 (1997).

[11] M. Metsälä, S. Yang, O. Vaittinen, D. Permogorov, and L. Halonen, Chem. Phys. Lett. **346**, 373 (2001).

[12] S. M. Hu, A. Campargue, Z. Y. Wu, Y. Ding, A. W. Liu, and Q. S. Zhu, Chem. Phys. Lett. **372**, 659 (2003).

[13] A. A. Istratova and O. F. Vyvenko, Rev. Sci. Instrum. **70**, 1233 (1999).

[14] D. Halmer, G. von Basum, P. Hering, and M. Mürtz, Rev. Sci. Instrum. **75**, 2187 (2004).

[15] M. Mazurenka, R. Wada, A. J. L. Shillings, T. J. A. Butler, J. M. Beames, and A. J. Orr-ewing, Appl. Phys. B **81**, 135 (2005).

[16] L. S. Rothman, D. Jacquemart, A. Barbe, D. C. Benner, M. Birk, L. R. Brown, M. R. Carleer, C. C. Jr, K. Chance, L. H. Coudert, V. Dana, V. M. Devi, J. M. Flaud, R. R. Gamache, A. Goldman, J. M. Hartmann, K. W. Jucks, A. G. Maki, J. Y. Mandin, S. T. Massie, J. Orphal, A. Perrin, C. P. Rinsland, M. A. H. Smith, J. Tennyson, R. N. Tolchenov, R. A. Toth, J. V. Auwera, P. Varanasi, and G. Wagner, J. Quant. Spectrosc. Radiat. Trans. **96**, 139 (2005).

[17] M. I. E. Idrissi, J. Liévin, A. Campargue, and M. Herman, J. Chem. Phys. **110**, 2074 (1999).

[18] Y. Kabbadj, M. Herman, G. D. Lonardo, L. Fusina, and J. W. C. Johns, J. Mol. Spectorsc. **150**, 535 (1991).

[19] J. V. Auwera, J. Mol. Spectorsc. **201**, 143 (2000).

[20] R. R. Gamache, R. L. Hawkins, and L. S. Rothman, J. Mol. Spectorsc. **142**, 205 (1990).

[21] L. S. Rothman, R. L. Hawkins, R. B. Wattson, and R. R. Gamache, J. Quant. Spectrosc. Radiat. Trans. **48**, 537 (1992).